

pubs.acs.org/joc Article

Catalytic Effects of Ammonium and Sulfonium Salts and External Electric Fields on Aza-Diels—Alder Reactions

Cyndi Qixin He, Ching Ching Lam, Peiyuan Yu, Zhihui Song, Maggie Chen, Yu-hong Lam, Shuming Chen, and K. N. Houk*



Cite This: J. Org. Chem. 2020, 85, 2618-2625



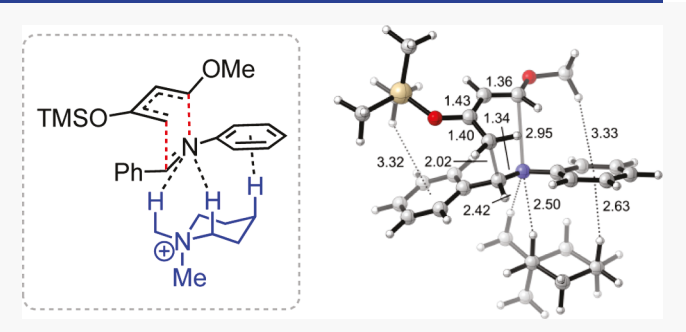
ACCESS

III Metrics & More

Article Recommendations

Supporting Information

ABSTRACT: The mechanism of the aza-Diels—Alder reaction catalyzed by tetraalkylammonium or trialkylsulfonium salts is explored with density functional theory. Favorable electrostatic interactions between the dienophile and the charged catalyst stabilize the highly polar transition state, leading to lower free energy barriers and higher dipole moments. Endo selectivity is predicted for both uncatalyzed and catalyzed systems. We also computationally evaluate the effects of oriented external electric fields (EEFs) on the same aza-Diels—Alder reaction, demonstrating that very strong EEFs would be needed to achieve the catalytic strength of these cationic catalysts.



INTRODUCTION

External electric fields (EEFs) are being explored with great interest as a means to lower chemical reaction barriers (Figure 1). To achieve catalysis, the EEF must be oriented to

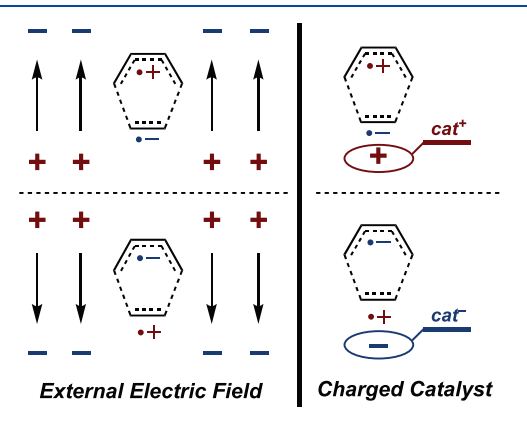


Figure 1. EEFs and charged catalysts most likely to stabilize polar Diels-Alder TSs.

maximize favorable Coulombic interactions with a polar transition state (TS). In the 1990s, Wilcox's studies of ion-pair effects on reaction rates and selectivities demonstrated how electrostatic fields could influence the rates of reactions with polar TSs,² including cycloadditions.^{2c,g} More recently, theoretical studies have demonstrated the potential of electrostatic catalysis to enhance reaction rates and selectivities,³ and a number of experimental examples in addition to Wilcox's have emerged, including the use of ion pairs to alter

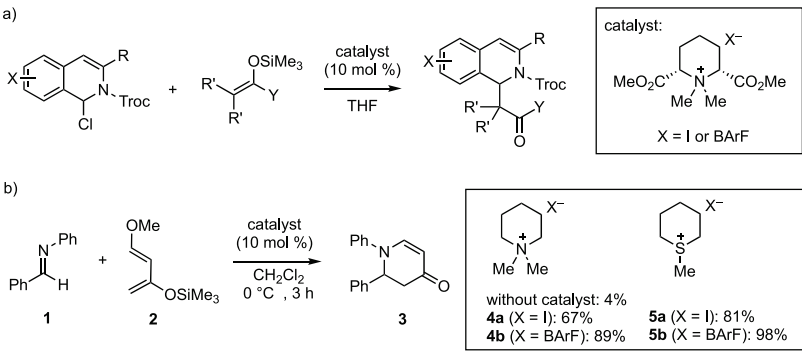
gold-catalyzed cyclizations^{3g,h} and the application of oriented electric fields on Diels—Alder and other reactions.⁴ Currently, most methods involve the application of strong EEFs in conjunction with molecular immobilization through surface chemistry techniques.⁴ An alternative approach is to use ionic catalysts to generate intense local oriented fields in the vicinity of the reactants (Figure 1).^{2,5} This approach is akin to enzymatic catalysis, which often relies on the electrostatic effects of strategically located charged or polar functional groups.⁶

In 2015, Maruoka and co-workers demonstrated tetraalky-lammonium salt catalysis in Mannich-type reactions (Scheme 1a). Shortly after, the authors reported the application of tetraalkylammonium and trialkylsulfonium salts as catalysts for the aza-Diels—Alder reactions between imine 1 and Danishefsky's diene 2 (Scheme 1b). The yield for desilylated aza-Diels—Alder adduct 3 was improved from 4% without the catalyst to 67% with 4a. Replacing the iodide counterion in 4a with the noncoordinating BArF anion further improved the yield to 89%. Trialkylsulfonium salts were more effective catalysts for this transformation than tetraalkylammonium salts. NMR titration experiments suggested association of the onium catalysts with the imine (dienophile), but no further evidence was obtained regarding the detailed reaction mechanism or the origins of catalysis. We performed a

Received: December 22, 2019 Published: December 31, 2019



Scheme 1. Mannich and Aza-Diels-Alder Reactions Catalyzed by Ammonium and Sulfonium Salts



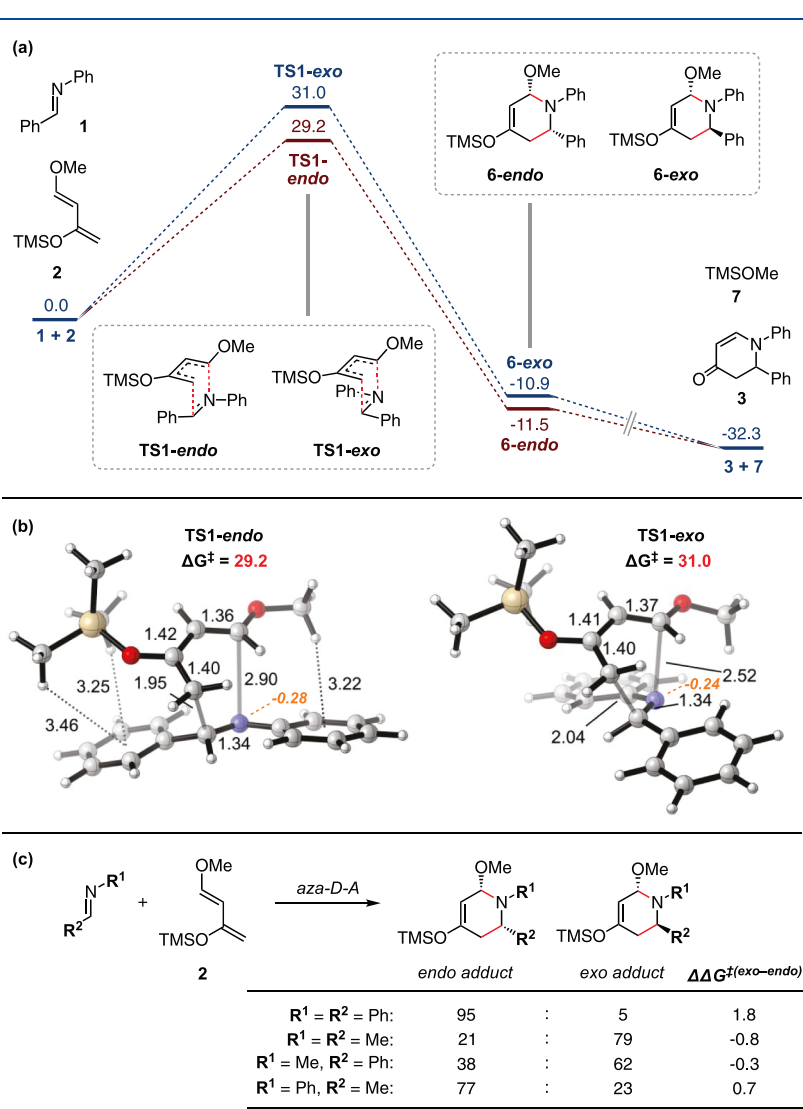


Figure 2. (a) Free energy profile of the aza-Diels—Alder reaction between imine 1 and Danishefsky's diene 2. Interatomic distances are in Å. Energies are in kcal/mol. (b) Calculated TSs for the aza-Diels—Alder reaction between 1 and 2. (c) Calculated endo/exo adduct ratios for the aza-Diels—Alder reaction of 2 with differently substituted imines.

computational study with density functional theory (DFT) quantum mechanics to elucidate the mechanism of the aza-Diels—Alder reaction between 1 and 2 and provide insight into how the onium catalysts lower the reaction barriers. The simple structures of the onium catalysts also facilitated a comparison of rate effects to that predicted for EEFs.

COMPUTATIONAL METHODS

DFT calculations were performed using Gaussian 09, revision D.01. Geometry optimizations and frequency calculations were performed at the ω B97X-D/6-31G(d) level of theory with the conductor-like polarizable continuum model (CPCM) using dichloromethane (ε = 8.9) to incorporate solvation effects. A pruned (99,590) grid (specified by the keyword int = ultrafine) was used for optimizations to minimize directional variations in calculated free energy

corrections. ¹² Thermal contributions to free energies were calculated from vibrational frequencies using the quasi-rigid rotor harmonic oscillator approach of Grimme ¹³ and Head-Gordon's enthalpy corrections. ¹⁴ All optimized geometries were verified by frequency computations as minima or first-order saddle-point structures. Single-point energy calculations on the optimized geometries were computed at the ω B97X-D/6-311+G(d,p), CPCM (dichloromethane) level of theory. EEF effects on single-point electronic energies were calculated using the "field = $M \pm N$ " keyword on molecular geometries optimized in the absence of EEFs. Conformational searches were carried out in MacroModel ¹⁵ and Spartan '16 ¹⁶ using the MMFFs force field, and DFT reoptimizations were performed on all conformers within a 10 kcal/mol cutoff. All 3D renderings of stationary points were generated using CYLview. ¹⁷

■ RESULTS AND DISCUSSION

Uncatalyzed Aza-Diels-Alder Reaction. Figure 2a shows the computed free energy profile of the uncatalyzed aza-Diels-Alder reaction between imine 1 and Danishefsky's diene 2. The free energy barrier is 29.2 kcal/mol for the endo pathway, and the exo pathway is 1.8 kcal/mol higher in energy. These barriers correspond to a very slow process under the reaction conditions, in good agreement with the experimentally observed low yield (4%) of the product. Desilylation of adduct 6 is highly exergonic by 20.8 kcal/mol or more to yield the stable enone product 3, with the elimination of one stereocenter. Both TS1-endo and TS1-exo have geometries characteristic of a concerted but asynchronous reaction, with the forming C-C bonds at 2.0 Å and forming C-N bonds at 2.5-2.9 Å (Figure 2b). The favored endo pathway is more asynchronous, with a larger negative Hirshfeld charge (-0.28)on the imine nitrogen at the TS.

Aza-Diels—Alder reactions typically show exo selectivity because of repulsive electrostatic $n-\pi$ interactions between the nitrogen lone pair and the diene π system (the exo-lone-pair effect). To probe the origin of the unusual endo selectivity of this reaction, we calculated the endo/exo ratios for aza-Diels—Alder reactions between 2 and imines with different substituents (Figure 2c). When both of the imine's phenyl rings are substituted by methyl groups, the reaction has a moderate exo preference. With a phenyl substituent in either the R¹ or R² position, the intrinsic exo selectivity is lowered or reversed. These results suggest that the endo selectivity is due to favorable electrostatic CH··· π interactions between the imine phenyl rings and substituents on the Danishefsky's diene.

Effect of Charged Catalysts and EEFs. Early in our study, we found that commonly used implicit solvent models such as solvent model density (SMD) and CPCM were not adequate for calculating free energies of complexation between imine 1 and charged ammonium or sulfonium catalysts. Though experimental NMR data show exergonic complex formation (Scheme 2), SMD and CPCM solvent models predicted these complexation to be 2–3 kcal/mol uphill at all tested levels of theory (see Supporting Information). As a result, we elected to use experimentally determined ΔG values for the complexation processes while studying the ammonium- and sulfonium-catalyzed aza-Diels—Alder reactions.

The calculated geometries of lowest-energy complexes between 1 and charged -onium catalysts are shown in Figure 3. Short interaction distances are observed between the imine nitrogen and the hydrogens α to the heteroatom on the catalyst, involving favorable electrostatic interactions. These

Scheme 2. Experimental Free Energies of Complexation (in kcal/mol) between Charged Ammonium and Sulfonium Catalysts and Imine Dienophile 1 of Benzhydryl Chloride

(a)
$$\bigoplus_{Me}^{N} Me$$
 \bigoplus_{BArF}^{Ph} \bigoplus_{CI}^{Ph} $\bigoplus_{AG = -0.7 (\pm 0.1)}^{Ph}$ \bigoplus_{H}^{Ph} \bigoplus_{BArF}^{Ph} \bigoplus_{BArF}^{Ph} \bigoplus_{BArF}^{Ph} $\bigoplus_{AG = -0.8 (\pm 0.1)}^{Ph}$ $\bigoplus_{AG = -0.8 (\pm 0.1)}^{Ph}$ \bigoplus_{BArF}^{Ph} \bigoplus_{BArF}^{Ph}

interaction distances are shorter in the sulfonium–imine complex, consistent with the higher acidity of the sulfonium ion. In addition, electrostatic $CH\cdots\pi$ interactions involving the imine phenyl substituents may contribute to the stabilities of these complexes.

Figure 4a shows the free energy profile of the ammoniumcatalyzed aza-Diels-Alder reaction between 1 and 2. We explored the free cation because the most effective salt, with the BArF counterion, is expected to have weak anion association. More strongly coordinating anions (e.g., halides) are found to give less effective catalysis.8 The free energy barrier for the catalyzed reaction is 25.2 kcal/mol, which is 4.0 kcal/mol lower than for the uncatalyzed system. The calculated intrinsic reaction coordinate (IRC) of TS2-endo confirms that the mechanism remains concerted but asynchronous, with no intervening potential energy surface (PES) minima. Both forming bonds (C-C at 2.02 Å, C-N at 2.95 Å) are longer than in the uncatalyzed TS1-endo, indicating an earlier TS (Figure 4b). The magnitude of the endo preference (2.0 kcal/ mol) is largely unchanged from the uncatalyzed system (1.8 kcal/mol), consistent with the observation that the same favorable CH $\cdots\pi$ interactions between 1 and 2 still distinguish the endo TS from the exo. In both TS2-endo and TS2-exo, the CH bonds α to the ammonium N are close to the partially negative imine nitrogen, consistent with the fact that the positive charge on the alkyl ammonium ion is mainly distributed around the α -CHs. ²⁰ The distances between the imine nitrogen and the partially charged α hydrogens on the catalyst significantly shorten in the TSs compared to 9, indicating stronger catalyst-dienophile association due to more favorable Coulombic interactions accompanying charge transfer from the diene to the dienophile.

The sulfonium-catalyzed aza-Diels—Alder reaction between 1 and 2 was calculated to have a barrier of 25.4 kcal/mol (Figure 5a), with the endo TS being preferred over the exo by 1.6 kcal/mol (Figure 5b). The calculated IRC for TS3-endo shows that the mechanism moves further in the stepwise direction under sulfonium catalysis, with a very shallow PES minimum detected between the two bond formation events. Attempts to optimize this PES minimum structure as an intermediate failed, with the geometry collapsing to the aza-Diels—Alder product instead. This result indicates that the formation of the second bond is essentially barrierless on the PES, although an entropic intermediate can be expected to exist on the free energy surface. The sulfonium ion is better at stabilizing the polar TSs, in agreement with the higher product yields obtained with sulfonium catalysts (Scheme 1).

The dipole moment vectors (defined here as negative toward positive) of uncatalyzed TSs TS1-endo and TS1-exo

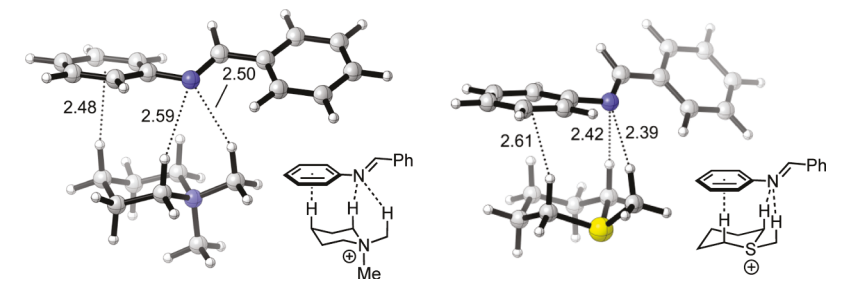


Figure 3. Calculated lowest-energy structures of complexes between imine 1 and charged catalysts. Interatomic distances are in Å.

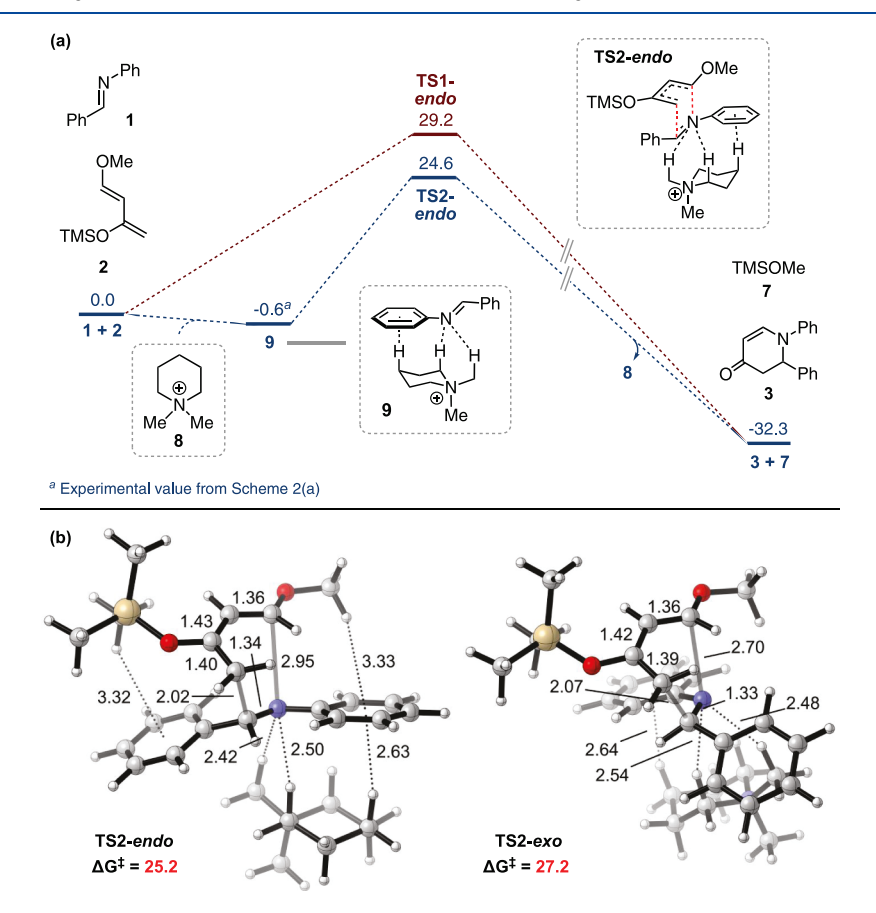


Figure 4. (a) Free energy profile of the aza-Diels—Alder reaction between 1 and 2 catalyzed by ammonium 8. Interatomic distances are in Å. Energies are in kcal/mol. (b) Calculated TSs for the aza-Diels—Alder reaction catalyzed by ammonium 8.

are shown in Figure 6a. TS1-endo has a larger dipole moment, in line with its more polar and asynchronous nature. We calculated the dipole-cation interaction energy between these TSs and a monovalent cation (Figure 6b), 22 assuming an interaction distance r of 5.6 Å from the center of the cationic charge to the center of the TS dipole.²²⁻²⁴ For the more asynchronous and polarizable TS1-endo, the maximum interaction energies are predicted to be 1.6 kcal/mol, which is qualitatively in agreement with the 101 to 102 rate acceleration observed experimentally with cationic catalysts. The largest interaction energies are encountered at $\theta = 0^{\circ}$ (maximum destabilizing effect) and 180° (maximum stabilizing effect). This result is consistent with our observation that in the calculated TSs, the positively charged nitrogen or sulfur centers of the catalysts typically prefer a θ angle very close to the 180° that maximizes the dipole-cation stabilizing effect.

Favorable dipole-cation interactions are expected to polarize the TS and increase the dipole moment. Indeed,

when the charged catalysts are excluded from the TS geometries, we calculated a significant increase in the dipole moments of the diene—dienophile fragments compared to the uncatalyzed TS (Figure 7).

To estimate the strength of oriented EEFs required to produce catalytic effects comparable to these charged onium catalysts, we calculated the free energy barriers and TS dipole moments under a range of EEF strengths, with the fields oriented either parallel or antiparallel to the TS dipole moment vectors (Figure 8). The results show that the exo TS exhibits higher sensitivity to the applied EEFs, although the endo preference is maintained throughout the EEF range we examined, which covered the range discussed in Coote et al.'s study of the effect of an oriented electric field on a Diels—Alder reaction rate. When the EEF applied in the Coote et al. study was increased from -0.05 to -0.75 V/nm, a 4.4-fold increase in measured rate was observed, similar to their calculation of a 0.2 kcal/mol lowering of activation barrier for

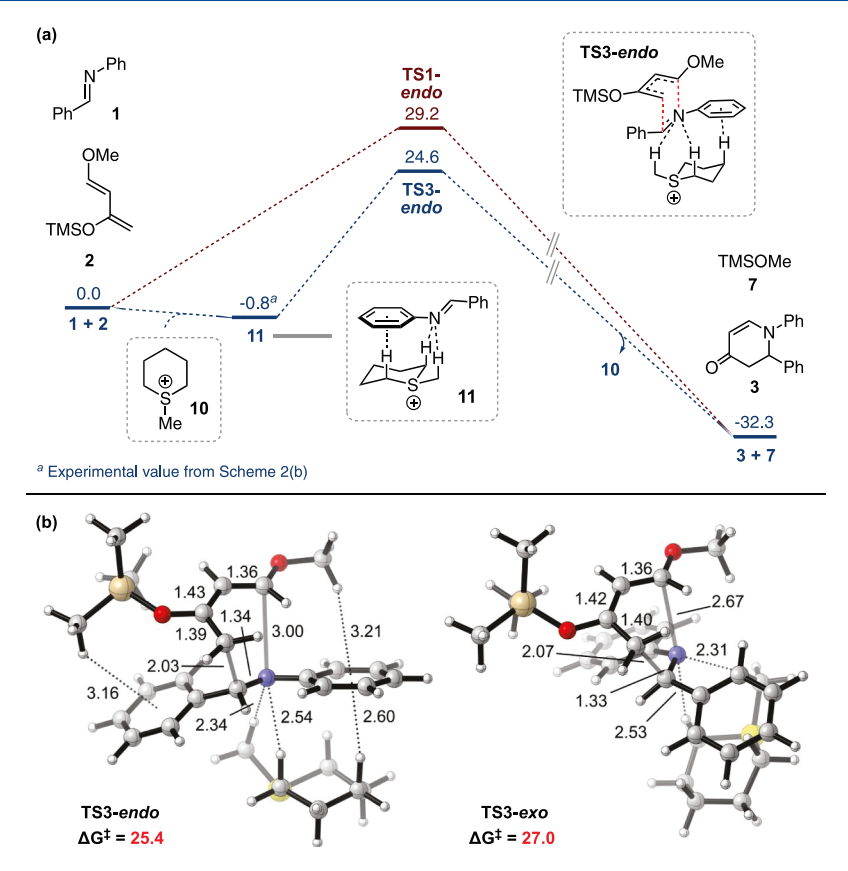


Figure 5. (a) Free energy profile of the aza-Diels—Alder reaction between 1 and 2 catalyzed by sulfonium 10. Interatomic distances are in Å. Energies are in kcal/mol. (b) Calculated TSs for the aza-Diels—Alder reaction catalyzed by sulfonium 10.

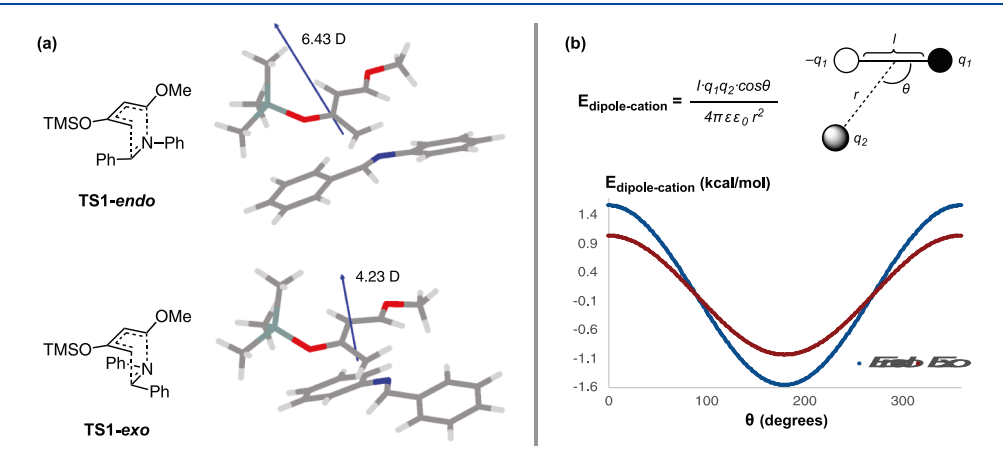


Figure 6. (a) Dipole moment vectors for uncatalyzed aza-Diels—Alder TSs. (b) Plot of dipole—cation interaction energies for uncatalyzed aza-Diels—Alder TSs TS1-endo and TS1-exo.

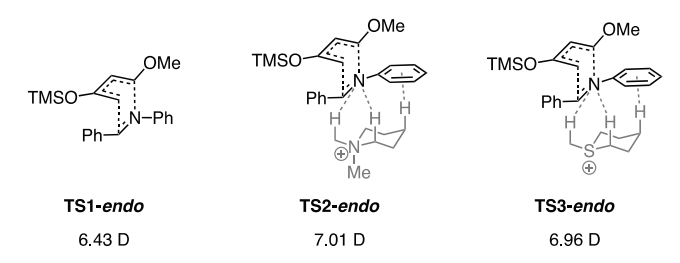


Figure 7. Calculated dipole moments of diene—dienophile fragments in aza-Diels—Alder TSs.

this type of voltage change.^{4a} As the free energy barriers are reduced, we find that the TSs become more polarized with

larger dipole moments (Figure 8). This polarization effect is also stronger for the more sensitive exo TS. At an EEF strength of 1.3 V/nm, the endo TS is stabilized by \sim 1.7 kcal/mol, similar in magnitude to the maximum dipole—cation interaction energy achieved at a distance of 5.6 Å (Figure 6b).

CONCLUSIONS

We have explored computationally the effect of ammonium and sulfonium catalysts on aza-Diels—Alder reactions with highly polar TSs. The catalysts are predicted to significantly lower the reaction free energy barriers by as much as 4 kcal/mol that would provide a several hundredfold increase in rate, while the impact on endo/exo selectivity was small. The origin

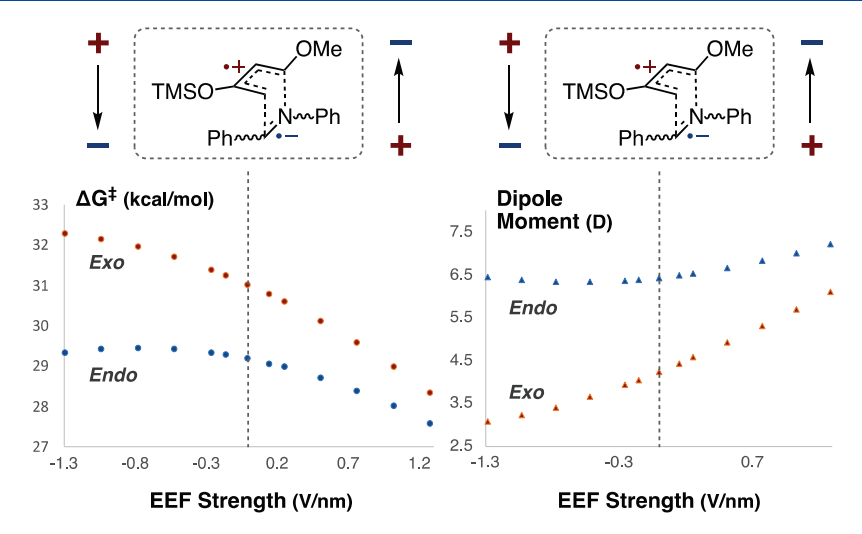


Figure 8. Calculated free energy barriers and TS dipole moments for the aza-Diels—Alder reaction between 1 and 2, with EEFs applied parallel (or antiparallel) to the dipole moment vectors shown in Figure 6a.

of catalysis is attributed to favorable electrostatic interactions between the cationic catalysts and the developing negative charges on the dienophile in the TSs. As the free energy barriers are lowered, the TSs also became more polarized with larger dipole moments. Unfortunately, only yields of reaction, not reaction rates, have been measured for these reactions to date, so that a quantitative comparison of calculations and experiment is not possible. We show that intense local fields generated by the ammonium and sulfonium ions are comparable in catalytic strength to the strongest EEFs currently being applied in electrostatic catalysis. This chemical approach, demonstrated in the work of Wilcox² and Kanan, ^{3g,h} is easily implemented in the synthetic laboratory. Our work highlights the great potential of charged catalysts and ion pairs as a scalable and practical approach to the electrostatic catalysis of reactions with polar TSs.

ASSOCIATED CONTENT

Supporting Information

The Supporting Information is available free of charge at https://pubs.acs.org/doi/10.1021/acs.joc.9b03446.

Computational details, energies, and cartesian coordinates of computed structures (PDF)

AUTHOR INFORMATION

Corresponding Author

K. N. Houk — University of California, Los Angeles, California; orcid.org/0000-0002-8387-5261; Email: houk@chem.ucla.edu

Other Authors

Cyndi Qixin He – University of California, Los Angeles, California

Ching Ching Lam – Imperial College London, London, U.K.

Peiyuan Yu — University of California, Los Angeles, California; o orcid.org/0000-0002-4367-6866

Zhihui Song — University of Maryland, College Park, Maryland

Maggie Chen – University of California, Los Angeles, California Yu-hong Lam — University of California, Los Angeles, California; orcid.org/0000-0002-4946-1487 Shuming Chen — University of California, Los Angeles, California; orcid.org/0000-0003-1897-2249

Complete contact information is available at: https://pubs.acs.org/10.1021/acs.joc.9b03446

Notes

The authors declare no competing financial interest.

ACKNOWLEDGMENTS

The authors are grateful to the National Science Foundation (grant CHE-1764328) for financial support of this research. Calculations were performed on the Hoffman2 cluster at the University of California, Los Angeles, and the Extreme Science and Engineering Discovery Environment (XSEDE), which is supported by the National Science Foundation (grant OCI-1053575). C.C.L. thanks the Imperial College Bursary Scheme for funding. S.C. thanks Dr. Jukka Väyrynen for helpful discussions.

REFERENCES

(1) (a) Shaik, S.; Mandal, D.; Ramanan, R. Oriented Electric Fields as Future Smart Reagents in Chemistry. *Nat. Chem.* **2016**, *8*, 1091–1098. (b) Shaik, S.; Ramanan, R.; Danovich, D.; Mandal, D. Structure and Reactivity/Selectivity Control by Oriented-External Electric Fields. *Chem. Soc. Rev.* **2018**, *47*, 5125–5145. (c) Welborn, V. V.; Ruiz Pestana, L.; Head-Gordon, T. Computational Optimization of Electric Fields For Better Catalysis Design. *Nat. Catal.* **2018**, *1*, 649–655.

(2) (a) Smith, P. J.; Wilcox, C. S. The chemistry of synthetic receptors and functional group arrays. 13. The intramolecular salt effect. J. Org. Chem. 1990, 55, 5675–5678. (b) Smith, P. J.; Wilcox, C. S. The Chemistry of Functional Group Arrays. Electrostatic Catalysis and the "Intramolecular Salt Effect. Tetrahedron 1991, 47, 2617–2628. (c) Smith, P. J.; Soose, D. J.; Wilcox, C. S. The Intramolecular Salt Effect. An Acrylate Ester Bearing an Ion Pair Shows Enhanced Rates and Stereoselectivity in a Nitrone Cycloaddition. J. Am. Chem. Soc. 1991, 113, 7412–7414. (d) Smith, P. J.; Reddington, M. V.; Wilcox, C. S. Ion Pair Binding by a Urea in Chloroform Solution. Tetrahedron Lett. 1992, 33, 6085–6088. (e) Smith, P. J.; Kim, E.-i.; Wilcox, C. S. Substrate-Specific Catalysis by Ion Pairs. Angew. Chem., Int. Ed. Engl. 1993, 32, 1648–1650. (f) Kim, E.-i.; Paliwal, S.; Wilcox, C. S. Measurements of Molecular Electrostatic Field Effects in Edge-

- to-Edge Aromatic Interactions and CH- π Interactions with Implications for Protein Folding and Molecular Recognition. *J. Am. Chem. Soc.* **1998**, 120, 11192–11193. (g) Raposo, C.; Wilcox, C. S. The Intramolecular Salt Effect in Chiral Auxiliaries. Enhanced Diastereoselectivity in a Nitrile Oxide Cycloaddition via Rational Transition Stable Stabilization. *Tetrahedron Lett.* **1999**, 40, 1285–1288.
- (3) (a) Shaik, S.; de Visser, S. P.; Kumar, D. External Electric Field Will Control the Selectivity of Enzymatic-Like Bond Activations. J. Am. Chem. Soc. 2004, 126, 11746-11749. (b) Hirao, H.; Chen, H.; Carvajal, M. A.; Wang, Y.; Shaik, S. Effect of External Electric Fields on the C-H Bond Activation Reactivity of Nonheme Iron-Oxo Reagents. J. Am. Chem. Soc. 2008, 130, 3319-3327. (c) Lai, W.; Chen, H.; Cho, K.-B.; Shaik, S. External Electric Field Can Control the Catalytic Cycle of Cytochrome P450cam: a QM/MM Study. J. Phys. Chem. Lett. 2010, 1, 2082-2087. (d) Meir, R.; Chen, H.; Lai, W.; Shaik, S. Oriented Electric Fields Accelerate Diels-Alder Reactions and Control the Endo/Exo Selectivity. ChemPhysChem 2010, 11, 301-310. (e) Gryn'ova, G.; Coote, M. L. Origin and Scope of Long-Range Stabilizing Interactions and Associated SOMO-HOMO Conversion in Distonic Radical Anions. J. Am. Chem. Soc. 2013, 135, 15392-15403. (f) Gryn'ova, G.; Marshall, D. L.; Blanksby, S. J.; Coote, M. L. Switching Radical Stability by pH-Induced Orbital Conversion. Nat. Chem. 2013, 5, 474-481. (g) Lau, V. M.; Gorin, C. F.; Kanan, M. W. Electrostatic Control of Regioselectivity via Ion Pairing in a Au(I)-Catalyzed Rearrangement. Chem. Sci. 2014, 5, 4975-4979. (h) Lau, V. M.; Pfalzgraff, W. C.; Markland, T. E.; Kanan, M. W. Electrostatic Control of Regioselectivity in Au(I)-Catalyzed Hydroarylation. J. Am. Chem. Soc. 2017, 139, 4035-4041. (i) Wang, Z.; Danovich, D.; Ramanan, R.; Shaik, S. Oriented-External Electric Fields Create Absolute Enantioselectivity in Diels-Alder Reactions: Importance of the Molecular Dipole Moment. J. Am. Chem. Soc. 2018, 140, 13350-13359.
- (4) For recent experimental examples, see: (a) Aragonès, A. C.; Haworth, N. L.; Darwish, N.; Ciampi, S.; Bloomfield, N. J.; Wallace, C. G.; Diez-Perez, I.; Coote, M. L. Electrostatic Catalysis of a Diels-Alder Reaction. *Nature* **2016**, *531*, 88–91. (b) Che, F.; Gray, J. T.; Ha, S.; McEwen, J.-S. Improving Ni Catalysts Using Electric Fields: A DFT and Experimental Study of the Methane Steam Reforming Reaction. *ACS Catal.* **2017**, *7*, 551–562. (c) Akamatsu, M.; Sakai, N.; Matile, S. Electric-Field-Assisted Anion– π Catalysis. *J. Am. Chem. Soc.* **2017**, *139*, 6558–6561. (d) Huang, X.; Tang, C.; Li, J.; Chen, L.-C.; Zheng, J.; Zhang, P.; Le, J.; Li, R.; Li, X.; Liu, J.; Yang, Y.; Shi, J.; Chen, Z.; Bai, M.; Zhang, H.-L.; Xia, H.; Cheng, J.; Tian, Z.-Q.; Hong, W. Electric Field–Induced Selective Catalysis of Single-Molecule Reaction. *Sci. Adv.* **2019**, *5*, No. eaaw3072.
- (5) (a) Aitken, H. M.; Coote, M. L. Can Electrostatic Catalysis of Diels—Alder Reactions Be Harnessed With pH-Switchable Charged Functional Groups? *Phys. Chem. Chem. Phys.* **2018**, *20*, 10671—10676. (b) Blyth, M. T.; Coote, M. L. A pH-Switchable Electrostatic Catalyst for the Diels—Alder Reaction: Progress toward Synthetically Viable Electrostatic Catalysis. *J. Org. Chem.* **2019**, *84*, 1517—1522.
- (6) (a) Warshel, A. Electrostatic Basis of Structure-Function Correlation in Proteins. *Acc. Chem. Res.* 1981, 14, 284–290. (b) Warshel, A.; Sharma, P. K.; Kato, M.; Xiang, Y.; Liu, H.; Olsson, M. H. M. Electrostatic Basis for Enzyme Catalysis. *Chem. Rev.* 2006, 106, 3210–3235. (c) Fried, S. D.; Boxer, S. G. Electric Fields and Enzyme Catalysis. *Annu. Rev. Biochem.* 2017, 86, 387–415. (d) Finkelmann, A. R.; Stiebritz, M. T.; Reiher, M. Electric-Field Effects on the [FeFe]-Hydrogenase Active Site. *Chem. Commun.* 2013, 49, 8099–8101.
- (7) Shirakawa, S.; Liu, S.; Kaneko, S.; Kumatabara, Y.; Fukuda, A.; Omagari, Y.; Maruoka, K. Tetraalkylammonium Salts as Hydrogen-Bonding Catalysts. *Angew. Chem., Int. Ed.* **2015**, *54*, 15767–15770.
- (8) (a) Kumatabara, Y.; Kaneko, S.; Nakata, S.; Shirakawa, S.; Maruoka, K. Hydrogen-Bonding Catalysis of Tetraalkylammonium Salts in an Aza-Diels—Alder Reaction. *Chem.—Asian J.* **2016**, *11*, 2126—2129. (b) Kaneko, S.; Kumatabara, Y.; Shimizu, S.; Maruoka,

- K.; Shirakawa, S. Hydrogen-Bonding Catalysis of Sulfonium Salts. *Chem. Commun.* **2017**, *53*, 119–122.
- (9) Frisch, M. J.; Trucks, G. W.; Schlegel, H. B.; Scuseria, G. E.; Robb, M. A.; Cheeseman, J. R.; Scalmani, G.; Barone, V.; Mennucci, B.; Petersson, G. A.; Nakatsuji, H.; Caricato, M.; Li, X.; Hratchian, H. P.; Izmaylov, A. F.; Bloino, J.; Zheng, G.; Sonnenberg, J. L.; Hada, M.; Ehara, M.; Toyota, K.; Fukuda, R.; Hasegawa, J.; Ishida, M.; Nakajima, T.; Honda, Y.; Kitao, O.; Nakai, H.; Vreven, T.; Montgomery, J. A., Jr.; Peralta, J. E.; Ogliaro, F.; Bearpark, M.; Heyd, J. J.; Brothers, E.; Kudin, K. N.; Staroverov, V. N.; Kobayashi, R.; Normand, J.; Raghavachari, K.; Rendell, A.; Burant, J. C.; Iyengar, S. S.; Tomasi, J.; Cossi, M.; Rega, N.; Millam, J. M.; Klene, M.; Knox, J. E.; Cross, J. B.; Bakken, V.; Adamo, C.; Jaramillo, J.; Gomperts, R.; Stratmann, R. E.; Yazyev, O.; Austin, A. J.; Cammi, R.; Pomelli, C.; Ochterski, J. W.; Martin, R. L.; Morokuma, K.; Zakrzewski, V. G.; Voth, G. A.; Salvador, P.; Dannenberg, J. J.; Dapprich, S.; Daniels, A. D.; Farkas; Foresman, J. B.; Ortiz, J. V.; Cioslowski, J.; Fox, D. J. Gaussian 09; Gaussian Inc.: Wallingford, CT, 2009.
- (10) Chai, J.-D.; Head-Gordon, M. Long-Range Corrected Hybrid Density Functionals with Damped Atom-Atom Dispersion Corrections. *Phys. Chem. Chem. Phys.* **2008**, *10*, 6615–6620.
- (11) (a) Barone, V.; Cossi, M. Quantum Calculation of Molecular Energies and Energy Gradients in Solution by a Conductor Solvent Model. *J. Phys. Chem. A* **1998**, *102*, 1995–2001. (b) Cossi, M.; Rega, N.; Scalmani, G.; Barone, V. Energies, Structures, and Electronic Properties of Molecules in Solution With the C-PCM Solvation Model. *J. Comput. Chem.* **2003**, *24*, *669*–*681*. (c) Takano, Y.; Houk, K. N. Benchmarking the Conductor-like Polarizable Continuum Model (CPCM) for Aqueous Solvation Free Energies of Neutral and Ionic Organic Molecules. *J. Chem. Theory Comput.* **2005**, *1*, 70–77.
- (12) Bootsma, A. N.; Wheeler, S. Popular Integration Grids Can Result in Large Errors in DFT-Computed Free Energies. **2019**. ChemRxiv. Preprint.
- (13) Grimme, S. Supramolecular Binding Thermodynamics by Dispersion-Corrected Density Functional Theory. *Chem.—Eur. J.* **2012**, *18*, 9955–9964.
- (14) Li, Y.-P.; Gomes, J.; Mallikarjun Sharada, S.; Bell, A. T.; Head-Gordon, M. Improved Force-Field Parameters for QM/MM Simulations of the Energies of Adsorption for Molecules in Zeolites and a Free Rotor Correction to the Rigid Rotor Harmonic Oscillator Model for Adsorption Enthalpies. *J. Phys. Chem. C* **2015**, *119*, 1840–1850.
- (15) MacroModel; Schrödinger, LLC: New York, 2016. (b) Watts, K. S.; Dalal, P.; Tebben, A. J.; Cheney, D. L.; Shelley, J. C. Macrocycle Conformational Sampling with MacroModel. J. Chem. Inf. Model. 2014, 54, 2680–2696.
- (16) Spartan'16; Wavefunction, Inc.: Irvine, CA.
- (17) Legault, C. Y. CYLview, 1.0b; Université de Sherbrooke, 2009, http://www.cylview.org.
- (18) (a) McCarrick, M. A.; Wu, Y. D.; Houk, K. N. Exo-Lone-Pair Effect on Hetero-Diels-Alder Cycloaddition Stereochemistry. *J. Am. Chem. Soc.* **1992**, *114*, 1499–1500. (b) McCarrick, M. A.; Wu, Y. D.; Houk, K. N. Hetero-Diels-Alder Reaction Transition Structures: Reactivity, Stereoselectivity, Catalysis, Solvent Effects, and the Exo-Lone-Pair Effect. *J. Org. Chem.* **1993**, *58*, 3330–3343. (c) Iafe, R. G.; Houk, K. N. Intramolecular Hetero-Diels-Alder Reactions of Imine and Iminium Dienophiles: Quantum Mechanical Exploration of Mechanisms and Stereoselectivities. *J. Org. Chem.* **2008**, *73*, 2679–2686.
- (19) Determined using NMR data from refs. Sa,b See Supporting Information for details.
- (20) Cannizzaro, C. E.; Houk, K. N. Magnitudes and Chemical Consequences of $R_3N^+-C-H\cdots O=C$ Hydrogen Bonding. *J. Am. Chem. Soc.* **2002**, *124*, 7163–7169.
- (21) Yang, Z.; Jamieson, C. S.; Xue, X.-S.; Garcia-Borràs, M.; Benton, T.; Dong, X.; Liu, F.; Houk, K. N. Mechanisms and Dynamics of Reactions Involving Entropic Intermediates. *Trends Chem.* **2019**, *1*, 22–34.

- (22) Anslyn, E. V.; Dougherty, D. A. Modern Physical Organic Chemistry; University Science Books, 2006.
- (23) The interaction distance of 5.6 Å is the measured dipole-cation distance r in **TS1-endo** and **TS1-exo**, where the position of the cation is taken to be the position of the ammonium nitrogen atom.
- (24) The equation shown in Figure 6b holds for r significantly larger than l. In the ammonium- and sulfonium-catalyzed systems, r and l are of approximately the same magnitude. We propose a more sophisticated treatment in the Supporting Information, which yields the same qualitative results and does not impact any of our conclusions.